Thermal Stability and Self-Assembly of Long α-Helices in the Gas Phase

Peter Palenčár, Tomáš Bleha

Polymer Institute, Slovak Academy of Sciences, 845 41 Bratislava, Slovakia

e-mail: peter.palencar@savba.sk

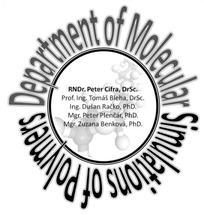

Abstract

Recent progress in experimental techniques such as ion mobility spectrometry coupled to mass spectrometry allows studying the conformation of flexible molecules including large biomacromolecules and synthetic polymers in the gas phase [1,2]. The adjustable temperature in experiment typically from 80 to 800 K allows the observation of thermal motion of floppy molecules or unfolding process of folded structures without dissociation of their covalent bonds. To interpret the indirect structure information from the gas phase experiments various computational techniques are applied [3]. The high temperature structure of typical nonpolar polymer is described as random coil. However, polymers such as polypeptides with highly developed hydrogen bonds network can sustain their secondary structure even at elevated temperatures.

Thermal stability of a single α-helix in the gas phase was studied by MD simulations at atomistic details [7]. The range of polymer chain length, *n* and temperature, *T* studied and the corresponding α-helical content, *Hα* is shown below in *Conclusions section* below. We observed highly ordered helical structures of Ala_n molecules at room temperature [4-7] and disordered and compacted non-random structures at *T* above 800 K. Surprisingly, high amounts of helices, turns and bends were found in chains at *T* >800 K, due to strong hydrogen bonding and of inter-residual attraction. The scaling exponents calculated for the radius of gyration, R_g vs chain length, *n* showed that the structure of Ala_n is contracted compared to a random coil - "crumpled" coil and condensed globule are observed. At room temperature, the self-assembly of an α-helix (*Hα* ~90 %) was observed. The straight α-helix is fragmented into antiparallel helices joined by short coils. The number of helices is dictated by *n*. The hairpin structures and helix bundles are found. The energy analysis reveals stability of hexagonal (6+1) structure.

Model and method

Model – α-helix represented by atomistic molecular model of polyalanine Ala_n of various lengths *n* from 20 to 300

Method – Molecular dynamics (MD) simulations in vacuum, leaping-frog integration, velocity rescale thermostat, Amber03 FF, NVT ensemble, 1.0 fs time step, annealing (see table below), H-bonds constrained by P-LINCS, switch function for vdW, cut-off 1.2 to 1.4 nm for L-J, cut-off 1.4 nm for short-range, Reaction-field-zero for Coulomb with 1.4 cut-off, 16 MD runs performed for each *n* using GROMACS and Yasara software. Secondary structure analysis done by do_dssp routine in Gromacs.

Annealing points		1.	2.	3.	4.	5.	6.	7.	8.	9.
T [K]		1500	**1500**	1200	**1200**	900	**900**	550	300	**300**
t [ns]	*n* =20, 30	0	10	15	25	65	75	160	170	175
	n =40, 60, 80	0	10	15	25	65	75	245	270	275
	n ≥100	0	10	15	25	65	75	525	570	575

The list of annealing points applied in MD simulations for three chain length regions. Highlighted are the annealing points of four constant temperature segments of MD.

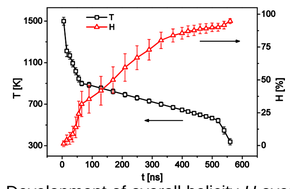

Development of overall helicity *H* over time in a relation to a change of temperature *T* of a single 575 ns-long MD trajectory of Ala_{100}.

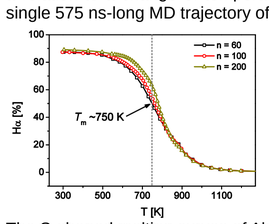

The S-shaped melting curves of Ala_{60}, Ala_{100} and Ala_{200} corresponds to the transition of ordered helical structures at low *T* into compact globules and collapsed-coils at higher *T*.

RESULTS

Thermal Stability

T K	H_α %	$H_{3\text{-}10}$ %	Turns %	Bends %	Coils %	R_g nm
1500	0.18	1.24	11.84	37.07	48.94	2.16
1200	0.89	3.78	17.51	34.16	42,13	1.71
900	13.17	16.48	29.00	18.43	21.19	1.39
800	37.78	18.44	26.38	7.72	8.96	1.40
700	67.19	10.92	14.97	2.66	4.11	1.50
600	80.33	6.33	8.62	1.51	3.17	1.49
500	85.65	4.20	6.29	0.97	2.87	1.46
300	87.34	4.49	4.88	0.65	2.64	1.44

The content (in %) of the secondary structure elements of Ala_{100} and its radius of gyration R_g as a function of *T*.

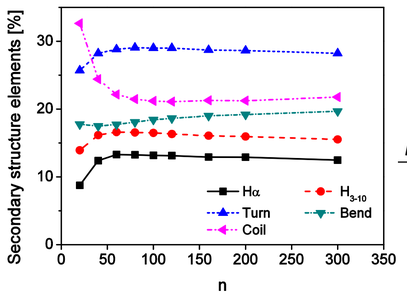

Fig. 1. The population of the secondary structure elements in equilibrium conformations of Ala_n at 900 K.

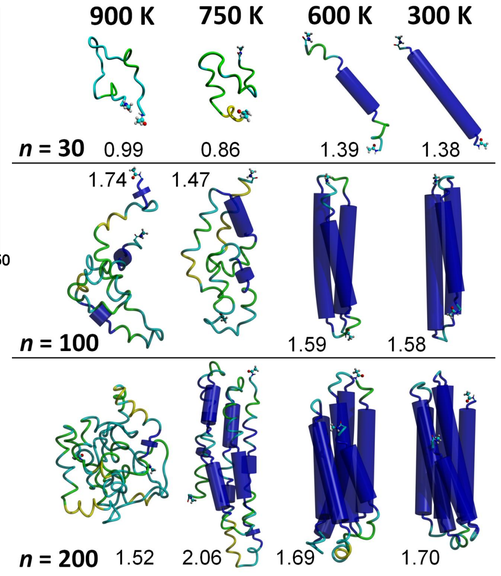

Fig. 4. Development of the helical order and of alignment of helical fragments in $(Ala)_n$ on cooling.

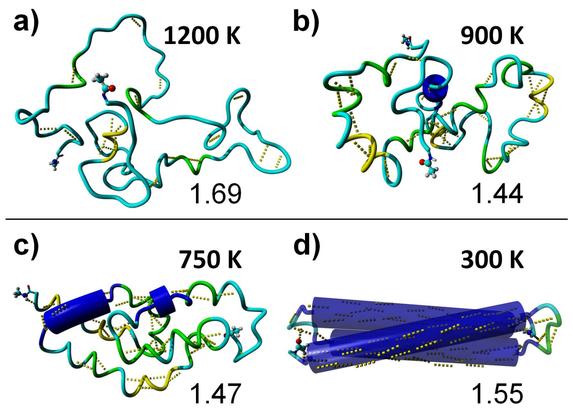

Fig. 2. Snapshots of representative conformations of $(Ala)_{100}$. The corresponding R_g (in nm) are given. The α-helices are shown as blue cylinders, and 3_{10}-helices as yellow tubes. The H-bonds are depicted as dashed lines.

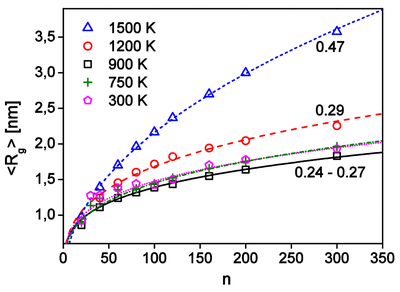

Fig. 3. The plot of the radius of gyration R_g as a function of the length *n*. The slopes *γ* of the power-law relation $R_g \approx A_o\, n^{\gamma}$ are obtained by the least-square fit.

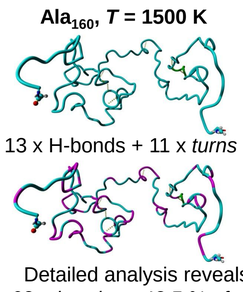

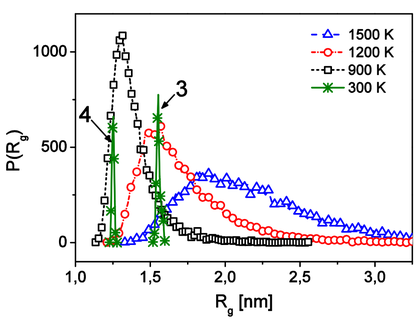

Fig. 5. The distribution function of the radius of gyration $P(R_g)$ in Ala_{100}. For two peaks at 300 K the number of helices in helix bundles, n_H = 3 and 4, is shown.

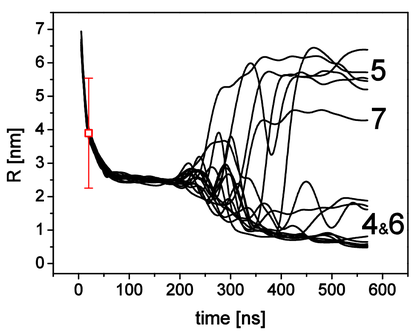

Fig. 6. The individual trajectories of end-to-end distance *R* of Ala_{200}. In the range 200-300 ns the zone of incipient nucleation of individual helix bundles is discernible.

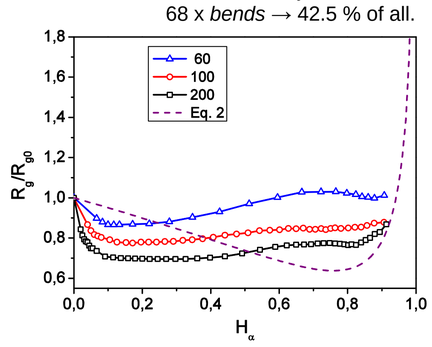

Fig. 7 The plot of the ratio of R_g relative to the value at zero helicity R_{g0} for Ala_n as a function of the α-helical content H_α. Prediction by $R_g/R_{g0} = [(1\text{-}H) + \kappa^2 H(H+1)/(1-H)]^{0.5}$ with $\kappa^2 = 0.03$ is shown by dashed line.

Self-Assembly at 300 K

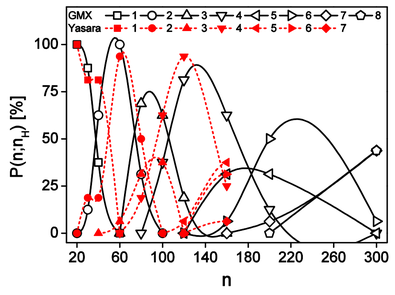

Fig. 8 The probability distributions $P(n;n_H)$ of the number of α-helices n_H as a function of *n* computed by Gromacs (open symbols) and Yasara (solid).

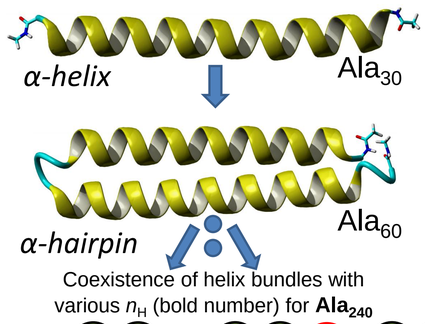

Coexistence of helix bundles with various n_H (bold number) for **Ala_{240}**

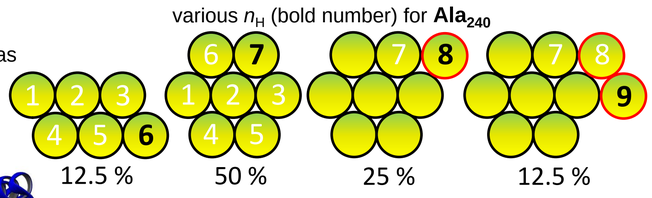

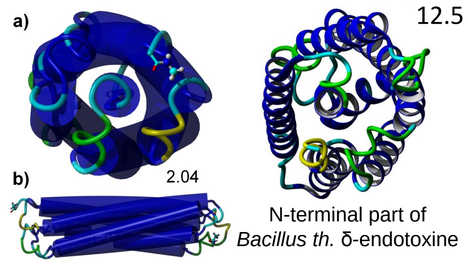

N-terminal part of *Bacillus th.* δ-endotoxine

Fig. 9 Representative hexagonal (6+1) structure of Ala_{300} at 300 K. a) Top view b) Side view revealing spatial organization of the helices.

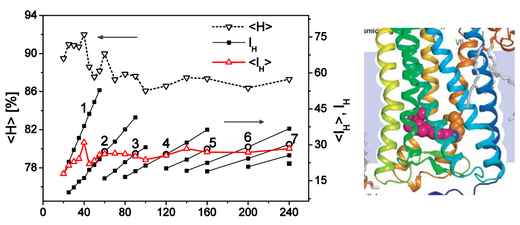

Fig. 10 The computed average length of helices, l_H ~28 residues, excellently matches the data for the span of transmembrane protein helices.

Conclusions

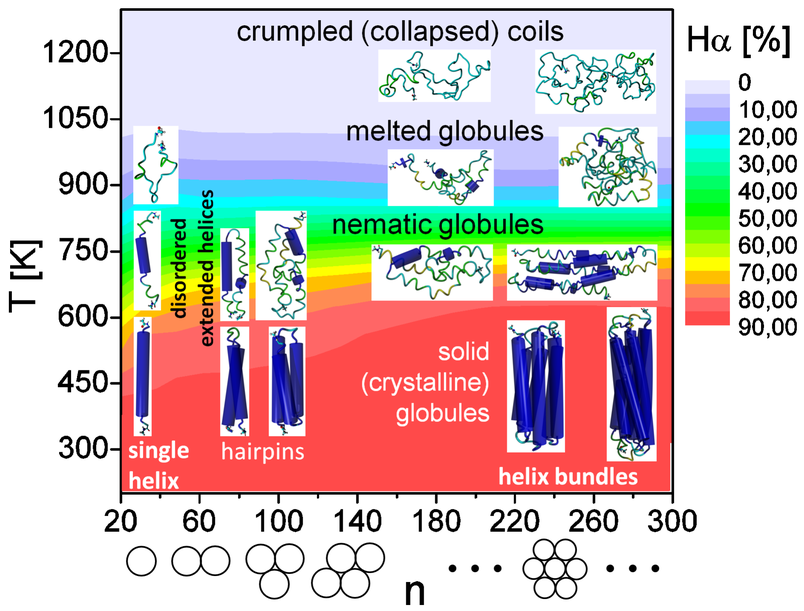

Fig. 11. The conformational state diagram of Ala_n as a function of *T* and chain length *n*. The content of α-helices H_α is given by a contour plot. The representative conformations are sketched for each region on the state diagram. The projection of helical bundles formed at low *T* is outlined along the abscissa.

The structure of α-helix is extremely thermally stable!

due to strong hydrogen bonding and of inter-residual attraction (Fig. 2 & 4)
high amounts of helices, turns and bends were found in chains at *T* >800 K (Fig. 1)

The structure of high *T* Ala_n is contracted compared to a random coil!

the scaling exponents of the radius of gyration, R_g vs chain length, *n* are small (Fig. 3 & 7)
"crumpled" coil and condensed globule are observed (Fig. 11)

Long Ala_n chains has the ability to self-assembly! (Fig. 6)

at room *T*, hairpin structure (*n* ~60) and helix bundles for *n* >60 are observed (Fig. 9 & 11)
perfect match with experimental data (Fig. 10), the number of helices n_H dictated by *n* (Fig. 8 & 11)

Reasons for Self-Assembly

Hydrogen bonds at the termini

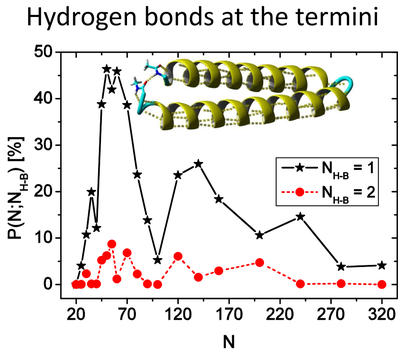

Zero, one ($N_{H\text{-}B}$ = 1) or two ($N_{H\text{-}B}$ = 2) hydrogen bonds (H-B) are found at Ala_n chain ends. The highest abundance of structures with one H-B is found among chains with *n* ~55 and *n* ~140.

Dipol-dipol interactions of adjacent helices

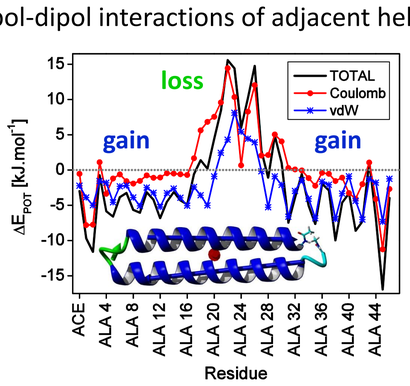

Energy gain along adjacent helices of Ala_n chain due to vdW attractions between them and energy loss in a short non-helical loop due to disruption of some of the Coulomb interactions. The helix dipoles are shown as thick arrows.

2D-hexagonal packing of helix bundles

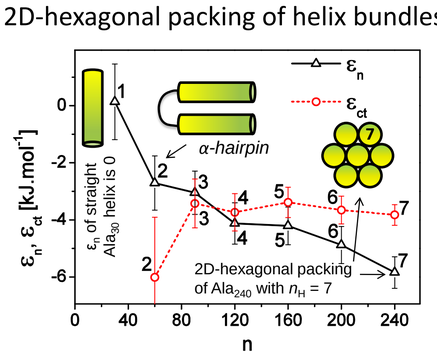

The stabilization energy ε_n of a bundle of the optimal chain length *n* normalized per number of Ala residues and the contact energy ε_{ct} as a function of chain length *n* at 303 K (see Ref. 5 for details).

[1] K. Breuker, F. W. McLafferty, *Proc.Natl.Acad.Sci.USA* 105:18145 (2008) **[2]** T. Wyttenbach, M. T. Bowers, *Top. Curr. Chem.* 225:207 (2003) **[3]** T. Mayer, V. Gabelica, H. Grubmuller, M. Orezco, DOI: 10.1002/wcms.1130 **[4]** P. Palenčár, T. Bleha, *Macromol. Theor. Simul.* 19:488 (2010) **[5]** P. Palenčár, T. Bleha, *Comp. Theor. Chem.* 1006:62 (2013) **[6]** P. Palenčár, T. Bleha, *J. Mol. Model.* 17:2367 (2011) **[7]** P. Palenčár, T. Bleha, *Polymer* 54:4955 (2013)

Acknowledgment: This work was supported by grants APVV-0451-11 and by VEGA grants No. 2/0079/12 and 2/0093/12.